

EVALUATION OF EFFECTIVE MECHANICAL PROPERTIES OF COMPLEX MULTIPHASE MATERIALS WITH FINITE ELEMENT METHOD

Mohamed said BOUTAANI¹, Salah MADANI², Kamel FEDAOUI³,
Toufik KANIT⁴

Prediction of effective properties for multiphase composite is very important not only to analysis and optimization of material performance, but also to new material designs. In this paper, the effective elastic property of some complex particulate composites is analyzed and compared with numerical results, demonstrating the validity of the proposed approach. We propose the equivalent morphology concept for the numerical homogenization of random composites. In this study, this concept is extended for complex material. A home script based on Python codes is made to automate the generating of Representative volume element with various volume fraction.

Keywords: Representative volume element, Computational homogenization, Finite element modeling.

1. Introduction

Heterogeneous materials are made of a mixing between inclusions phase and matrix. As a result of a non-uniform mixing, during the dispersion of inclusions in the matrix, we are getting microstructures with complex shape. For example, this is the case of microstructures of Concrete, Voronoi mosaics and the case of microstructures of composite materials with aggregates. Several numerical homogenization techniques, based on the notion of the Representative Volume Element (RVE), are used to estimate the effective linear elastic properties, of three dimensional (3D) microstructures.

In the literature, for describing the elastic behavior of composites many models exist [1, 2]. The prediction of the effective elastic properties of heterogeneous materials is based on the knowledge of relations between the microstructure and the macroscopic response.

¹ Prof., Laboratoire de Mécanique de Structures & Matériaux, Université de Batna 2, Algeria,
E-mail : poutasfr@yahoo.fr

² Prof., Laboratoire de Mécanique de Structures & Matériaux, Université de Batna 2, Algeria.

³ Prof., Laboratoire de Mécanique de Structures & Matériaux, Université de Batna 2, Algeria, e-mail : fedaouik@yahoo.fr

⁴ Prof., Laboratoire de Mécanique de Structures & Matériaux, Université de Batna 2, Algeria,

This has been achieved by using micromechanical models, which considered only the matrix and reinforcement properties and their volume fractions. The majority of analytical models and bounds do not take into account the influence of the particle shape on the effective properties. This can only be achieved by solving numerically the boundary value problem for a Representative Volume Element (RVE) of material [3, 4].

Several researchers have used the finite element method (FEM) to understand the effect of particles volume fractions on the mechanical behavior of composites [3, 4, 5, 6].

In this paper, the effect of phase shape on the effective linear elastic properties and on the RVE size, is investigated using FEM. A numerical homogenization technique, based on finite element simulations was used by applying periodic boundary conditions (PBC). Two different materials are considered, one with complex shapes for the second phase and the second material with spherical particle embedded into matrix. The equivalent morphology concept is proposed here to replace the complex shape two-phase material with a simple two-phase composite composed of spherical inclusions embedded into the matrix.

2. Computational homogenization

In this section, all elements and notations of numerical homogenization necessary to determine the effective elastic properties, using the methodology explained by [2] based on the FEM, are described.

2.1 Microstructures generating and elastic properties of phases

This work concerns the prediction of mechanical properties of two-phase composite materials by 3D numerical simulation. Simulations are performed using the finite element method coupled with a homogenization method. The generation algorithm of complex material is developed with a Python code [7], see figure 1. To simplify the calculations, simulations were performed for a RVE. The algorithm generates 3D complex material for a specified volume fraction, in a cubic region. The automated generation process will not stop until the volume fraction is satisfied. The morphology and technique of 3D microstructures generation is presented in this section. For each studied microstructure, many configurations with different form of the second phase are investigated. Each microstructure contains one population of second phase, randomly distributed in a continuous matrix. Different elastic properties are attributed to the two phases, in order to predict the effective elastic properties of composites. Table 1 represents the mechanical properties of each phase used for numerical computations. φ_1 is the volume fraction of the second phase and φ is the volume fraction of the matrix.

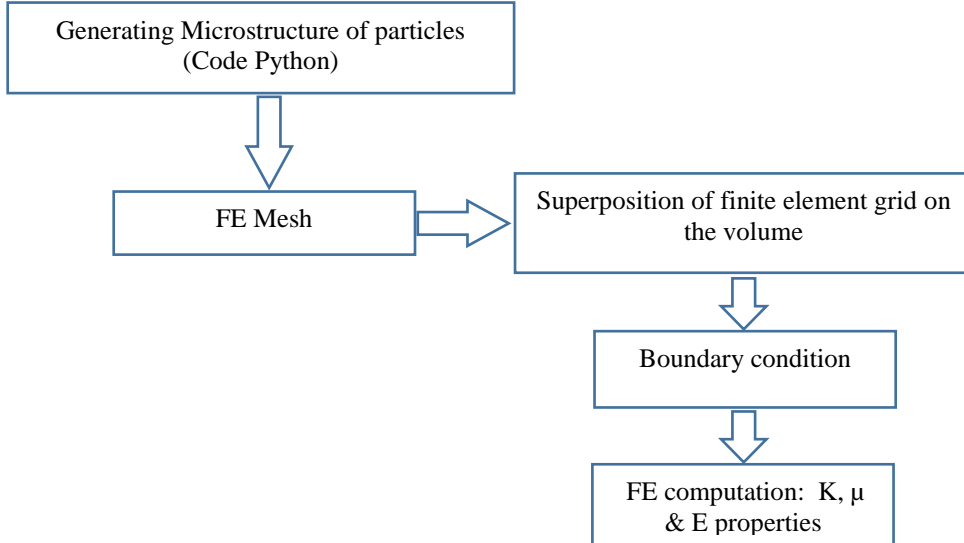


Fig 1: Process of numerical computation.

Table1

Cases of composites used for numerical computations.

Material	Case	Volume fraction for matrix and inclusions
Complex Two -Phase material	Case 1	$\varphi=95\%$, $\varphi_1=5\%$
	Case 2	$\varphi=90\%$, $\varphi_1=10\%$
	Case 3	$\varphi=80\%$, $\varphi_1=20\%$
	Case 4	$\varphi=70\%$, $\varphi_1=30\%$

Table2

Elastic properties of each phase used for numerical computations.

Phase	Matrix	Inclusion
Young modulus [MPa]	100	10
Poisson ratio	0.3	0.3

FE computations on volumes of different sizes extracted from the entire volume V were performed. The main advantage of this strategy is that it allows us to work on a sufficiently large volume for a low computational cost. Figure 2 presents an example of RVE of complex microstructure and a subdivision of this whole microstructure into images.

In all simulation, many realizations for the same volume fraction of material were generated to estimate the elastic properties. We note that the number of realizations from the small volume size V_1 to large one V_6 decrease. The different configurations with increasing sizes are summarized in Table 3.

Table 3

Cases of volume size used for numerical computations.

	<i>V1</i>	<i>V2</i>	<i>V3</i>	<i>V4</i>	<i>V5</i>	<i>V6</i>
<i>Volume size [px³]</i>	50*50*50	80*80*80	100*100*100	150*150*150	200*200*200	250*250*250
<i>Number of realizations</i>	30	30	10	8	5	5

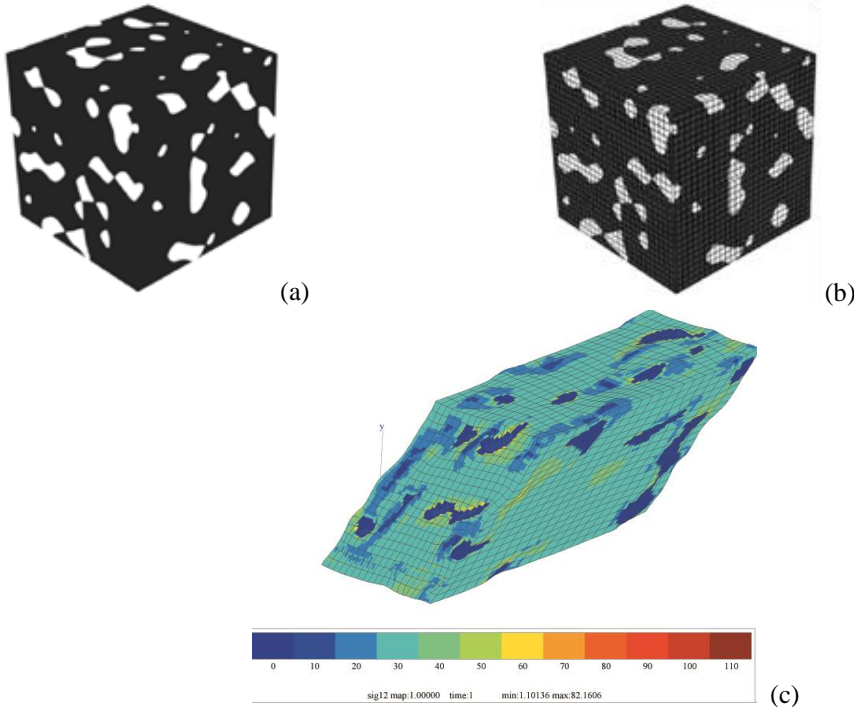


Fig. 2. Example of material used in this investigation, (a) material with 30%, (b) 3D mesh, c) shear strain.

2.2 Mesh generation and mesh density

A regular 3D finite element mesh is superimposed on the image of the microstructure using the so-called multi-phase element technique. This technique was developed in [2] and used for the homogenization of virtual or real images by several authors as [4, 8, 9, 10]. As a result of convergence, a good mesh density of quadratic 20 nodes elements and 27 integration points per one FE was adopted in all this investigation for all simulations, see Figure 3.

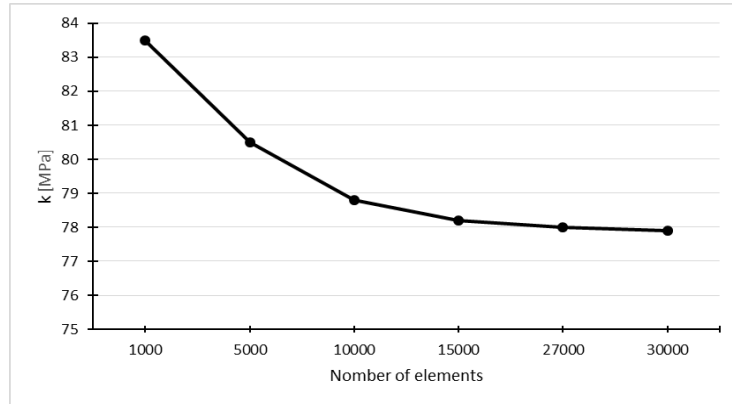


Fig. 3. Evolution of Bulk modulus as a function of the number of elements.

2.3 Boundary conditions

The homogenization theory is used for the numerical determination of effective linear elasticity properties. A volume element of a heterogeneous material is considered. Conditions are prescribed at its boundary in order to estimate its overall properties. The periodic boundary conditions are to be prescribed on individual volume element. These boundary conditions were used with prescribed values of strain tensor ε on individual volume element V . These conditions are defined by a displacement field over the outside contour ∂V as:

$$u = \varepsilon \cdot x + v \quad \forall x \in \partial V \quad (1)$$

The fluctuation v is periodic. It takes the same values at two homologous points on opposite faces of V . ε represents the macroscopic deformation and x the position vector.

For the PBC, to compute macroscopic bulk and shear moduli we take:

$$\varepsilon_k = \frac{1}{3} \begin{pmatrix} 1 & 0 & 0 \\ 0 & 1 & 0 \\ 0 & 0 & 1 \end{pmatrix} \quad \text{and} \quad \varepsilon_\mu = \frac{1}{2} \begin{pmatrix} 0 & 1 & 0 \\ 1 & 0 & 0 \\ 0 & 0 & 0 \end{pmatrix} \quad (2)$$

where ε_k and ε_μ are the macroscopic strain tensors used for computing k^{app} and μ^{app} respectively.

We define the following "apparent bulk and shear modulus" (k^{app} and μ^{app}):

$$k^{\text{app}} = \langle \sigma \rangle : \varepsilon_k = \frac{1}{3} \text{trace} \langle \sigma \rangle = \frac{1}{3} \langle \sigma_{11} + \sigma_{22} + \sigma_{33} \rangle \quad (3)$$

$$\mu^{\text{app}} = \langle \sigma \rangle : \varepsilon_\mu = \langle \sigma_{12} \rangle \quad (4)$$

where $\langle x \rangle$ is the average value x . σ_{11} , σ_{22} , σ_{33} , represent the principal stresses and σ_{12} the shear stress.

2.4 Hashin-Shtrikman bounds

The Hashin-Shtrikman bounds [11] are the tightest bounds possible from range of composite moduli for a two-phase material. Specifying the volume fraction of the constituent moduli allows the calculation of rigorous upper and lower bounds for the elastic moduli of any composite material. The so-called Hashin-Shtrikman bounds for the bulk, K , and shear moduli μ is given by:

$$k^{HS\pm} = k_1 + \frac{1 - P}{(k_2 - k_1)^{-1} + P \left(k_1 + \frac{4}{3} \mu_1 \right)^{-1}} \quad (5)$$

$$\mu^{HS\pm} = \mu_1 + \frac{1 - P}{(\mu_2 - \mu_1) + \frac{2P(k_1 + 2\mu_1)}{5\mu_1 \left(k_1 + \frac{4}{3} \mu_1 \right)}} \quad (6)$$

where P is the volume fraction of the inclusions, K_1 and K_2 are the bulk modulus of the inclusions and matrix respectively, μ_1 and μ_2 are the shear modulus of the inclusions and matrix respectively.

The upper bound is computed when ($K_2 > K_1$ and $\nu_2 > \nu_1$). The lower bound is computed by interchanging the indices in the equations.

3. Results and discussion

In this part, for the determination of the bulk and shear modulus of heterogeneous materials, a numerical technique with RVE notion developed in [2] is used. It consists in considering different realizations of random and complex microstructures in order to obtain the effective properties. The RVE is the volume that allows the estimation of the effective property with one realization.

The size of the RVE and the effective property are obtained by variation of the volume size, see Table 3. From the obtained results, it appears that the size of RVE depend on the size of material investigated.

Figure 4, reported the variations of effective bulk and shear modulus in term of volume fraction for case 1. The results are compared to the HS bounds. The variation of effective elastic properties in term of volume fraction for all the cases of complex material are reported in Figure 5. For the low volume fraction 5% and 10% the RVE is located for small volume size compared with the other volume fraction 20 and 30%.

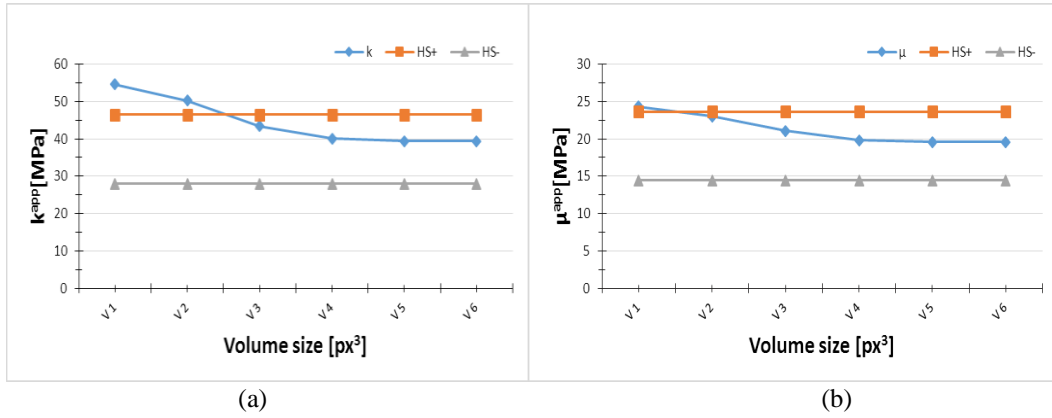


Fig 4. Variation of the bulk (a) and the shear modulus (b) with HS bounds in terms of volume size for case 1 of complex material.

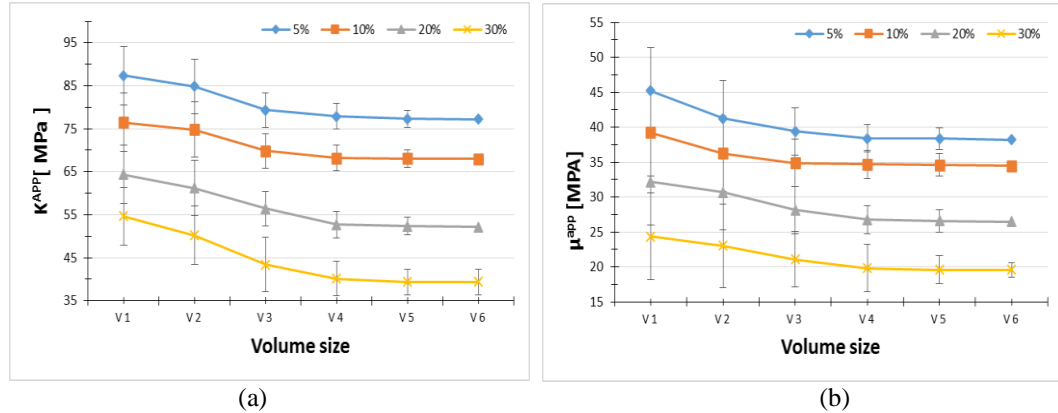


Fig 5. Variation of the bulk (a) and the shear modulus (b) in terms of volume size for four-volume fraction of complex material.

Table 4

RVE size from numerical computations.

Material	Case	RVE Size [pixel ³]
Complex material	Case 1	V3
	Case 2	V3
	Case 3	V4
	Case 4	V5

In Table 4, the size of RVE for all the cases study in this paper are reported.

4. Effect of volume fraction on effective elastic properties

Many authors have studied the effect of volume fraction on the effective elastic properties of composite materials. In order to investigate the effect of

volume fraction of second phase on the effective bulk and shear modulus, different volumes fractions of material were investigated, the effective bulk and shear modulus decrease with the increase of the volume fraction of inclusions and converge to the effective value for the RVE volume size, see Figure 5.

5. Equivalent morphology concept

In this section, we propose to replace a complex two phase material with a simple two-phase material. The second material is made of spherical inclusion embedded into the matrix. We make the assumption that the volume fraction is the same in the two configurations. The distribution of the inclusions is random. The Python script used for generating the complex material is adapted to generate the material with spherical particles. Two constraints were made to the distribution of spheres:

- The spheres do not overlap with each other
- The spheres do not collide with the cell walls (cube)

The three cases of generation spheres with three types of fraction (5%, 10%, 20% and 30%) are presented in Figure 6.

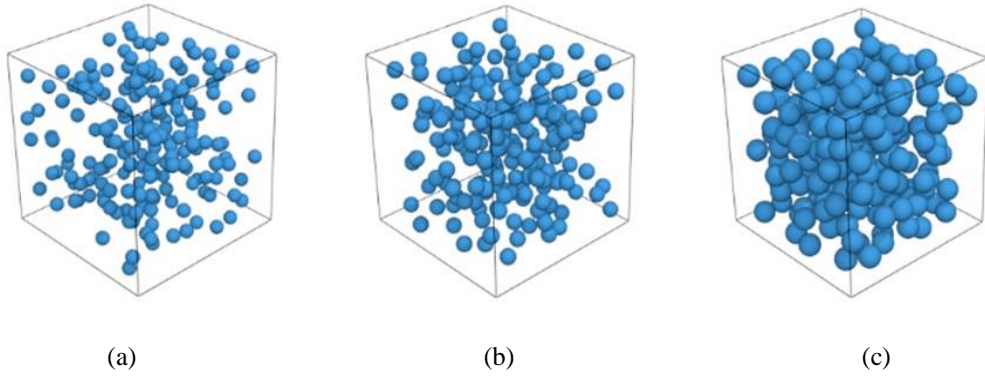


Fig 6. Generation of spherical particles for different volumes fraction, a) 5%, b) 10% and c) 20%.

The technique of generation of this microstructure containing random sphere packings is obtained with a *Python* code with *RSA* algorithm used in [12, 13, 14, 15, 16], see Fig. 1.

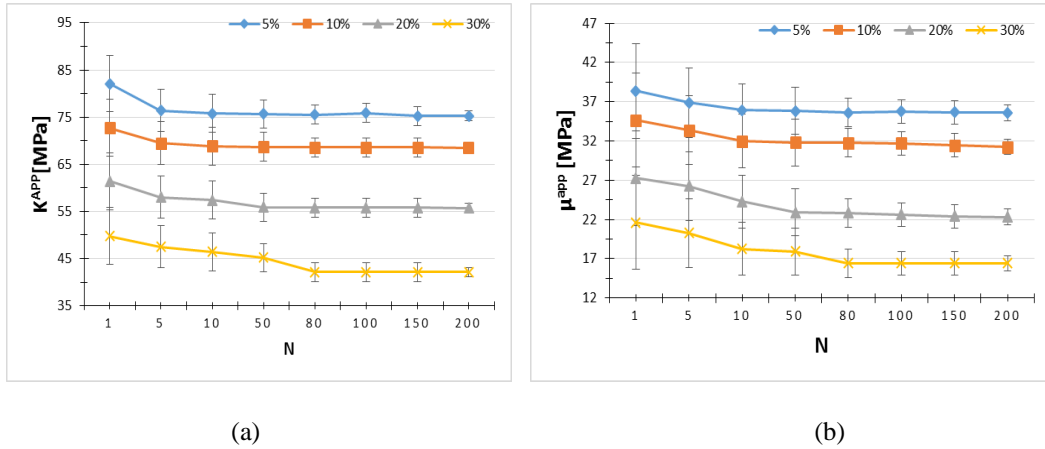


Fig 7. Variation of the bulk (a) and the shear modulus (b) in terms of volume size for composite for four-volume fraction of with spherical inclusions.

Figure 7 present the results of effective elastic properties of spherical inclusions in term of number of inclusions N for all the volume fractions.

The relative error between modulus of complex morphology and modulus of morphology with spherical inclusions should be calculated as:

$$\text{Relative error } (k) = (k_{\text{complex}} - k_{\text{spherical}})/k_{\text{complex}} \quad (7)$$

The relative error between modulus of complex morphology and modulus of morphology with spherical inclusions should be calculated as:

$$\text{Relative error } (\mu) = (\mu_{\text{complex}} - \mu_{\text{spherical}})/\mu_{\text{complex}} \quad (8)$$

Table 5

Numerical results for Bulk modulus for complex and spherical inclusion material and the HS bounds

Volume Fraction of inclusions (%)	k [MPa] complex material	k [MPa] spherical inclusion	HS-	HS+	Relative Error (%)
5	74.164	74.228	64.052	75.366	0.086
10	70.283	67.419	51.672	68.290	4
20	52.734	55.705	36.702	56.271	5.6
30	51.541	46.521	27.978	47.233	9.7

Table 6.

Numerical results for Shear modulus for complex and spherical inclusion material and the HS bounds

Volume Fraction of inclusions (%)	μ [MPa] complex material	μ [MPa] spherical inclusion	HS-	HS+	Relative Error (%)
5	35.138	35.220	30.917	35.539	0.2
10	31.968	33.244	25.640	32.823	4
20	26.895	27.306	18.742	27.922	1.5
30	22.351	30.331	14.432	25.241	35.7

According to the Figures 8 and 9, the curves of the effective elastic properties k and μ for the two morphologies converge and nearly equal. The error between the value of k and μ in the two cases are negligible for volumes fraction 5, 10 and 20%, see Table 5 and 6. For the volume fraction 30%, the origin of the difference (9.7% for bulk modulus and 35% for the shear modulus) is the height heterogeneity of material in the two morphologies. The error in (%) is calculated between effective modulus of complex morphology and morphology with spherical inclusions.

Using these results, we can deduce the concept of equivalent morphology, which allows us to replace the original morphology of complex two-phase material by another morphology named equivalent morphology just containing spheres, provided the volume fraction of the second phase in original morphology equals to the volume fraction of spherical particle one in its equivalent morphology. These two morphologies give the same effective elastic properties but not necessarily the same RVE.

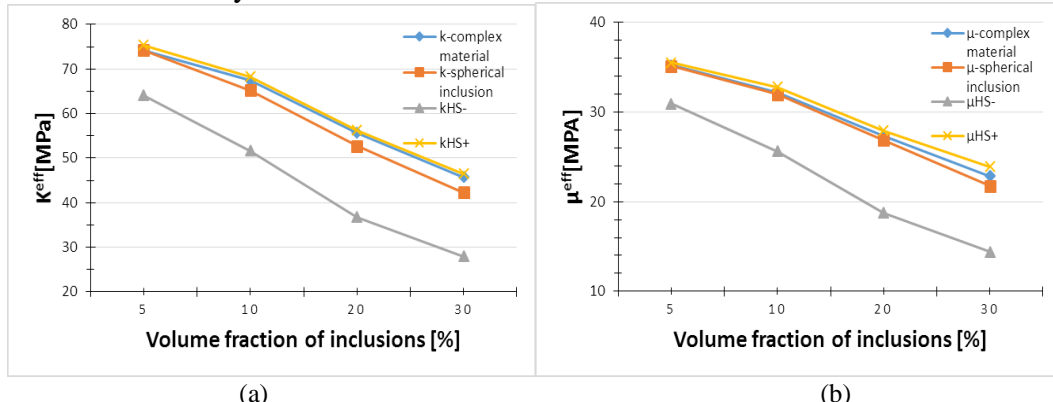


Fig 8. Variation of effective material properties for complex material with change in volume fraction and comparison with different analytical results: a), Bulk modulus, b) Shear modulus.

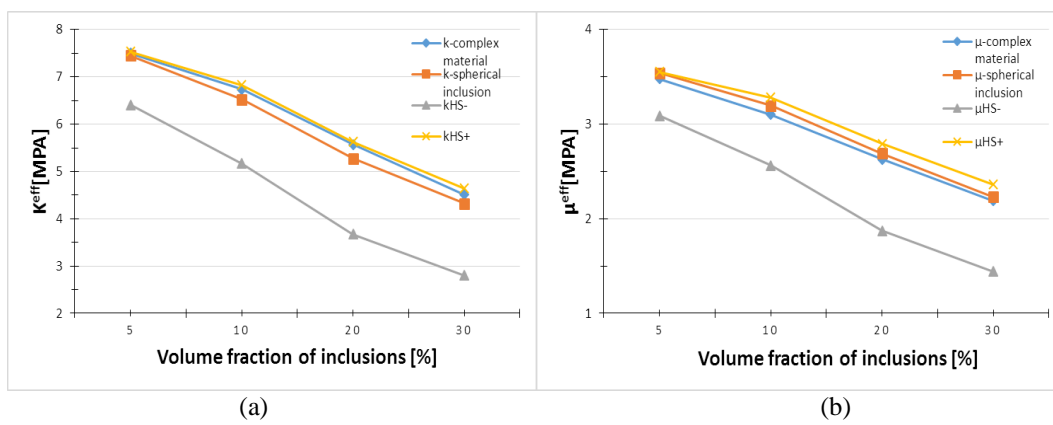


Fig 9. Variation of effective elastic properties with changing the volume fraction for the microstructure with spheres a) for bulk and (b) shear modulus.

6. Conclusions

A 3D cell model is used to predict the effective mechanical properties of two-phase complex material using homogenization techniques for different volume fractions. The numerical approach is based on the finite element method. Bulk and shear effective modulus have been calculated using a finite element model and compared with HS bounds.

The concept of equivalent morphology, which allows us to replace the original morphology of complex two-phase material by another morphology named equivalent morphology just containing spheres, is proposed to reduce the mesh time of complex microstructure and memory.

The numerical results demonstrate that the developed FE approach is very accurate and efficient for the analysis of 3D complex material. The present work has laid down a foundation for further applications of micro-mechanical finite element analysis for problems, such as an investigation of stress field in order to understand the onset and the development of inelastic behavior such as plastic deformation and possible damage. Furthermore, the proved reliability of the introduced FEM approach opens new possibilities to explore composites with arbitrary geometrical types of inclusions, which cannot be covered by most other homogenization methods.

R E F E R E N C E S

- [1]. *S. Kari, H. Berger and U. Gabbert*, Numerical evaluation of effective material properties of randomly distributed short cylindrical fiber composites, Computational Materials Science, vol. 39, 2007, pp.198-204
- [2]. *T. Kanit, S. Forest, I. Galliet, V. Mounoury and D. Jeulin*, Determination of the size of the representative volume element for random composites, statistical and numerical approach, Int. J. Solids Struct., vol. 40, 2003, pp. 3647–3679
- [3]. *Y.K. Khdir, T. Kanit, F. Zaïri and M. Nait-Abdelaziz*, A computational homogenization of random porous media: Effect of void shape and void content on the overall yield surface, European Journal of Mechanics - A/Solids, Elsevier, vol. 49, 2015, pp. 137-145
- [4]. *A. El Moumen, T. Kanit, A. Imad, and H. El Minor*, Effect of overlapping inclusions on effective elastic properties of composites, Mechanics Research Communications, vol. 53, 2013, pp. 24–30
- [5]. *A. El Moumen, T. Kanit, A. Imad and H. El Minor*, Computational thermal conductivity in porous materials using homogenization techniques: numerical and statistical approaches, Comput. Mater. Sci., vol. 97, 2015, pp. 148–158
- [6]. *A. El Moumen, T. Kanit , A. Imad and H. El Minor*, Effect of reinforcement shape on physical properties and representative volume element of particles reinforced composites: statistical and numerical approaches, Mech Mater, vol. 83, 2015, pp. 1–16
- [7]. Python code: <https://www.python.org/>
- [8]. *K. Fedaoui., S. Madani. and T. Kanit*, Prediction of effective thermal conductivity of heterogeneous random multi-phase composites, U.P.B. Sci. Bull., Series D, vol. 78, Iss. 3, 2016
- [9]. *N. Lippmann*, Comput. Mater. Sci., vol. 9, 1997, pp. 28–35

- [10]. *S. Forest*, Milieux continus généralisés et matériaux hétérogènes, Ecole des Mines, Paris, 2006.
- [11]. *Z. Hashin, S. Shtrikman*, A variational approach to the theory of the elastic behaviour of multiphase materials, *Journal of the Mechanics and Physics of Solids*, vol. 11, 1963, pp. 127-140
- [12]. *M. Pahlavan, H. Moussaddy and E. Ghossein*, Prediction of Elastic Properties in Polymer-Clay Nanocomposites: Analytical Homogenization Methods and 3D Finite Element Modeling, *Computational Materials Science*, vol. 79, 2013, pp. 206-215
- [13]. *S. Torquato*, Exact Expression for the Effective Elastic Tensor of Disordered Composites, *Phys. Rev. Lett.*, vol. 79, 1997, pp. 681-684
- [14]. *M. S. Boudaoui, S. Madani, T. Kanit and K. Fedaoui*, On the Homogenization of 2D Porous Material with Determination of RVE, *IJMME-IJENS*, vol. 16, no. 1, Feb. 2016, pp. 81-86
- [15]. *H. Moussaddy, D. Therriault and M. Lévesque*, Assessment of existing and introduction of a new and robust efficient definition of the representative volume element, *International Journal of Solids and Structures*, vol. 50, 2013, pp. 3817-3828
- [16]. *E. Ghossein and M. Lévesque*, A comprehensive validation of analytical homogenization models: The case of ellipsoidal particles reinforced composites, *Mechanics of Materials*, 75, pp. 135-150, 2014.